Solitons and the excitation spectrum of classical ferromagnetic chains with axial anisotropy

H. R. Jauslin and T. Schneider
IBM Zurich Research Laboratory, 8803 Rüschlikon—ZH, Switzerland
(Received 15 March 1982)

With the use of the molecular-dynamics technique and nonlinear spin-wave theory, we investigate the relevance of envelope solitons in dynamic form factors in classical one-dimensional Heisenberg models with axial anisotropy. We find that magnon bound-state contributions survive in the classical limit. Their main effects are a central peak, a bound-state resonance, and the removal of unphysical singularities. The correspondence between envelope solitons and magnon bound states as obtained by semiclassical quantization provides an interpretation of these effects as soliton features. Comparison with previous results for spin $\frac{1}{2}$ suggests that the structure of the dynamic form factors at finite temperature is essentially independent of the spin value.

I. INTRODUCTION

In recent years important progress has been achieved in the understanding of the excitation spectrum of one-dimensional (1D) systems. The development of the inverse-scattering technique (IST) has allowed the determination of the complete set of eigenmodes of a series of classical systems, including the Heisenberg and Landau-Lifshitz models.[1] These models are completely integrable and their eigenmodes can be classified in terms of linear modes and solitons. The corresponding quantum spin-$\frac{1}{2}$ Heisenberg and XYZ models on a lattice have been exactly diagonalized using the Bethe ansatz,[2] or the quantum version of the IST.[3–5]

However, the calculation of measurable quantities such as dynamic form factors still presents unsolved difficulties. Exact calculations have been performed only for some special cases, like the spin-$\frac{1}{2}$ XY model for all temperatures[6] and the axial anisotropic model at zero temperature.[7–10] For other anisotropies and finite temperatures numerical and approximate analytical methods have been developed.[10] We used the molecular-dynamics technique to calculate dynamic form factors for the classical axial anisotropic Heisenberg model, concentrating on variables specially adequate to detect soliton features. Nonlinear spin-wave theory in the classical limit was used to interpret the results and identify the different contributions.

While originally, investigation of 1D systems was motivated mainly by their mathematical properties and by their relative simplicity compared with higher dimensional ones, discovery of a series of quasi-one-dimensional magnetic substances has given them direct physical significance.[11–13] In this context the question arose to what extent the classical soliton eigenmodes have experimentally observable effects.[14,15] The main conditions for such effects are the following: Firstly, the quasi-one-dimensional system must be describable with enough accuracy by a 1D Heisenberg model with anisotropies (XYZ, Landau-Lifshitz models). Secondly, the classical approximation should be valid under the conditions where the soliton effects are to be observed. Since the solitons are defined only in the continuum model, a further requirement is that the soliton effects have a certain stability when one goes from the continuum to the lattice model. This can be expected, at least for some values of the parameters for which the discrete model is well approximated by the continuum one. Finally, the solitons should have clear-cut contributions in experimentally observable quantities: thermodynamic quantities, like the specific heat or the susceptibility, or dynamic form factors, which can be measured in neutron[11] or light scattering[16–18] experiments.

For the 1D ferromagnet $CsNiF_3$ in a field, which can be described by a Heisenberg model[11] with single-site easy-plane anisotropy (EPH), Mikeska[19] proposed a mapping to the sine-Gordon model, suggesting an interpretation of neutron scattering experiments[20] in terms of sine-Gordon solitons. Unfortunately, numerical studies on the EPH and the sine-Gordon systems showed that the validity of the mapping is limited to a small region in the parame-

ter space where three-dimensional ordering and quantum effects are important.[21,22]

In this paper we investigate the relevance of soliton features in dynamic form factors of Heisenberg ferromagnetic chains with single-site and exchange anisotropies of axial type. Their classical continuum version belongs to the class of Landau-Lifshitz models.[23] They are completely integrable, and their solutions can be classified in terms of linear modes and envelope solitons. The envelope solitons are traveling waves of permanent localized profile with an inner degree of freedom[24,25] whose form remains unchanged after collisions. They are similar to the breather solitons of the sine-Gordon system. The axial anisotropic models we consider, with boundary conditions $S^z(\pm\infty)=S$, do not have topological soliton solutions of the type of the sine-Gordon kinks. For a detailed discussion of the soliton solutions of the Landau-Lifshitz models see Refs. 23–25.

The corresponding classical discrete models are not expected to be completely integrable. However, for parameters close enough to the continuum limit the excitations can be interpreted using the continuum concepts. Moreover, we found that the soliton effects in some form factors remain essentially unchanged when some of the parameters are driven further away from the continuum limit. Although there are no strict solitons for these parameters, by a continuity argument one can interpret them as soliton features.

The quantum-mechanical spectrum of the axial anisotropic Heisenberg models is known to consist of magnons, multimagnon continua, and magnon bound states.[26–31] For the spin-$\frac{1}{2}$ model with anisotropic exchange of axial-type (AEH), the complete bound-state spectrum was obtained by Gochev.[26] For the (EAH), the spectrum was obtained through a mapping to a gas of bosons with attractive δ-function interactions.[28,29,32] The relation between the classical and the quantum elementary modes was established by applying semiclassical quantization procedures to the solutions of the classical equations.[28–31] The quantized linear modes and envelope solitons were identified with magnons and magnon bound states, respectively. We shall use this correspondence to identify the contributions of the envelope solitons in dynamic form factors.

The procedure is the following. We calculate the dynamical form factors numerically, using the molecular-dynamics (MD) technique. It consists of numerically solving the classical equations of motion for a large finite chain with periodic boundary conditions, using starting configurations chosen according to a canonical-ensemble distribution. The time-dependent correlation functions are obtained by averaging over the starting configurations.

In order to interpret these results and identify the different resonances, we use an approximative analytical calculation valid for low temperatures and becoming exact at $T=0$. We calculate quantum Green's functions, where the contributions of magnon and magnon bound states can be easily identified, and then take the classical limit. The bound-state resonances survive the classical limit, and according to the semiclassical correspondence, they can be identified as envelope soliton features.

II. DEFINITION OF THE SYSTEMS

We consider the following general form of the ferromagnetic Heisenberg Hamiltonian that includes the two types of anisotropy we shall investigate:

$$H=-J\sum_l\left[S_l^zS_{l+1}^z+\frac{1}{g}(S_l^xS_{l+1}^x+S_l^yS_{l+1}^y)\right]+h\sum_l S_l^z-D\sum_l S_l^{z^2}, \tag{1}$$

$$J>0,\quad D>0,\quad g>1\ .$$

In the quantum treatment (QM), the $\vec{S}_l$ are spin operators obeying the commutation relations

$$[S_l^\alpha,S_j^\beta]=i\hbar\epsilon^{\alpha\beta\gamma}\delta_{lj}S_l^\gamma\ . \tag{2}$$

We shall use the following nomenclature for the different choices of anisotropy parameters g and D: EAH is the easy-axis, single-site anisotropic exchange where $g=1$ and $D>0$; AEH is the anisotropic exchange of axial type where $1<g\leq\infty$ and $D=0$; $g=\infty$ corresponds to the Ising limit. A characteristic of these models is that the Hamiltonian commutes with the z component of the total spin $S_{\rm tot}^z$, which allows the classification of the eigenstates of H in terms of $S_{\rm tot}^z$. In the ground state all the spins are aligned parallel to the anisotropy axis. To establish the correspondence with the classical model[33,34] we define the normalized operator

$$\vec{s}=\frac{1}{\hbar\sqrt{S(S+1)}}\vec{S}\ , \tag{3}$$

which obeys the commutation relations

$$[s_l^\alpha,s_j^\beta]=i\epsilon^{\alpha\beta\gamma}\frac{\delta_{lj}}{\sqrt{S(S+1)}}s_l^\gamma\ . \tag{4}$$

In this notation, the Hamiltonian is

$$H=-J\hbar^2S(S+1)\sum_l\left[s_l^zs_{l+1}^z+\frac{1}{g}(s_l^xs_{l+1}^x+s_l^ys_{l+1}^y)\right]+\hbar\sqrt{S(S+1)}h\sum_l S_l^z-D\hbar^2S(S+1)\sum_l s_l^{z^2}\ . \tag{5}$$

The classical limit (cl) is defined as

$$S\to\infty,\quad \hbar\to0,\quad S\hbar=S_{\rm cl}=\text{const.} \tag{6}$$

In this limit, the commutators (4) are equal to zero. The spin operators go over to classical vectors of length $S\to\infty,\ \hbar\to0,\ S\hbar=S_{\rm cl}=\text{const}$.

$$H_{\rm cl}=-JS_{\rm cl}^2\sum_{l=1}^N\left[s_l^zs_{l+1}^z+\frac{1}{g}(s_l^xs_{l+1}^x+s_l^ys_{l+1}^y)\right]+hS_{\rm cl}\sum_{l=1}^N s_l^z-DS_{\rm cl}^2\sum_{l=1}^N s_l^{z^2}\ . \tag{7}$$

This expression shows that the dependence on the length of the classical spin is trivial, since it can be absorbed into the constants $JS_{\rm cl}^2$, $hS_{\rm cl}$, and $DS_{\rm cl}^2$.

The classical spin vectors $\vec{S}$ obey the equation of motion

$$\frac{d\vec{S}_l}{dt}=\vec{S}_l\wedge\tilde{J}(\vec{S}_{l+1}+\vec{S}_{l-1})+2\vec{S}_l\wedge\tilde{D}\vec{S}_l+\vec{S}_l\wedge\vec{h}\ , \tag{8}$$

$$\tilde{J}=\text{diag}(J/g,J/g,J),\quad \tilde{D}=\text{diag}(0,0,D)\ ,$$

obtained as the classical limit of the Heisenberg equation for the spin operators

$$\frac{d\vec{S}_l}{dt}=\frac{i}{\hbar}[H,\vec{S}_l]\ , \tag{9}$$

or directly from the Hamiltonian function (7) using the Poisson brackets[35]

$$\frac{d\vec{S}_l}{dt}=\{H,\vec{S}_l\}\ ,\qquad \{S_l^\alpha,S_j^\beta\}=-\epsilon^{\alpha\beta\gamma}\delta_{lj}S_l^\gamma\ . \tag{10}$$

When there is no possible confusion, we shall drop the notation cl.

In order to obtain the continuum limit of the model, we put into the interactions an explicit dependence on the lattice constant a, which is absorbed in the strength of the coupling constants[23]

$$J=\hat{J}/a,\quad 1/g=1-\delta a^2\ ,\qquad D=\hat{D}a,\quad h=\hat{h}a\ . \tag{11}$$

The Hamiltonian can be written up to constant terms as

$$H=\frac{\hat{J}}{2}\sum_l a\frac{(\vec{S}_l-\vec{S}_{l+1})^2}{a^2}-\frac{\hat{J}}{2}\sum_l a^3\delta\left[\frac{(S_l^x-S_{l+1}^x)^2}{a^2}+\frac{(S_l^y-S_{l+1}^y)^2}{a^2}\right]-\hat{J}\delta\sum_l aS_l^{z^2}-\hat{D}\sum_l aS_l^{z^2}+\hat{h}\sum_l aS_l^z\ . \tag{12}$$

Taking the continuum limit $a\to0$, $\sum_l a\to\int dx$, which according to (11) also implies a weak anisotropy limit, one obtains

$$H=\frac{\hat{J}}{2}\int dx\left[\frac{\partial\vec{s}}{\partial x}(x)\right]^2-(\hat{D}+\hat{J}\delta)\int dx\,[S^z(x)]^2+\hat{h}\int dx\,S^z(x)\ , \tag{13}$$

which is a special case of the Landau-Lifshitz model.[23] Thus in the continuum limit both the AEH and the EAH lead to the Landau-Lifshitz model. The continuum model should be a good approximation of the discrete model for long wavelengths and small anisotropies.

III. CORRELATION FUNCTIONS; GREEN'S FUNCTIONS

We shall concentrate on the following dynamic form factors:

$$S_{xx}(q,w)=\frac{1}{2\pi}\int dt\, e^{i\omega t}\langle S^x_{-q}(0)S^x_q(t)\rangle\ , \quad (14)$$

$$S^x_q=\frac{1}{\sqrt{N}}\sum_l e^{iql}S^x_l\ , \quad (15)$$

which probe the fluctation of one-spin deviations, and

$$S_{jj}(q,\omega)=\frac{1}{2\pi}\int_{-\infty}^{\infty} dt\, e^{i\omega t}\langle A^j_{-1}(0)A^j_q(t)\rangle\ , \quad (16)$$

$$A^j_q=\frac{1}{\sqrt{2N}}\sum_l e^{iql}(S^+_lS^+_{l+j}+S^-_lS^-_{l+j})\ . \quad (17)$$

S_{00} and S_{11} probe fluctuations of two-spin deviations located at the same and neighboring sites, respectively.

The dynamic form factors can be calculated from the corresponding Green's functions[36,37]

$$S_{BB}(q,\omega)=2G''_{BB}(q,\omega)\frac{1}{1-e^{-\beta\hbar\omega}}\ , \quad (18)$$

which in the classical limit become

$$S_{BB}(q,\omega)=2\frac{1}{\hbar}G''_{BB}(q,\omega)\frac{T}{\omega}\ . \quad (19)$$

We use the notations G' and G'' for the real and imaginary parts of G, respectively.

The Green's functions are defined as

$$G_{AB}(q,\omega)\equiv\langle\langle A;B\rangle\rangle=\frac{1}{2\pi}\int dt\, e^{i\omega t}G_{AB}(q,t)\ , \quad (20)$$

$$G_{AB}(q,t)=-i\Theta(t)\langle[A_q(t),B^\dagger_{-q}(0)]\rangle\ , \quad (21)$$

and obey the equation of motion

$$\hbar\omega\langle\langle A;B\rangle\rangle=\frac{\hbar}{2\pi}\langle[A_q(t=0),B^\dagger_{-q}(t=0)]\rangle+\langle\langle[A,H];B\rangle\rangle\ . \quad (22)$$

The spectral representation of the Green's function shows that its poles correspond to the elementary excitations of the system. The two-magnon spectrum can be determined by locating the poles of a two-magnon Green's function as S_{00} or S_{11}. At $T=0$, the equations of motion can be solved exactly.[7–9] There is a one-magnon excitation branch with dispersion

$$\omega_q=2JS\left[1-\frac{1}{g}\cos q\right]+2D(S-\tfrac{1}{2})+h\ . \quad (23)$$

The two-magnon spectrum consists of a continuum and one (AEH) or two (EAH) bound states. The top and bottom of the continuum are given by

$$\omega_{BC}=4JS\left[1-\frac{1}{g}\cos\frac{q}{2}\right]+4DS\left[1-\frac{1}{2s}\right]+2h\ , \quad (24)$$

$$\omega_{TC}=4JS\left[1+\frac{1}{g}\cos\frac{q}{2}\right]+4DS\left[1-\frac{1}{2s}\right]+2h\ . \quad (25)$$

IV. DYNAMIC FORM FACTORS AT $T>0$

To calculate the Green's functions at finite temperature, we use the Dyson-Maleev bosonization[38,39] of the spin operators, defined as

$$\begin{aligned} S^+_l&=S^x_l+iS^y_l=(2S)^{1/2}\hbar a^\dagger_l\left[1-\frac{a^\dagger_la_l}{2S}\right]\ ,\\ S^-_l&=S^x_l-iS^y_l=(2S)^{1/2}\hbar a_l\ ,\\ S^z_l&=\hbar(-S+a^\dagger_la_l)\ , \end{aligned} \quad (26)$$

where a_l are boson operators obeying the commutation relations

$$\begin{aligned} &[a_l,a^\dagger_j]=\delta_{lj}\ ,\\ &[a_l,a_j]=[a^\dagger_l,a^\dagger_j]=0\ . \end{aligned} \quad (27)$$

Their Fourier transform is defined by

$$\begin{aligned} a_l&=\frac{1}{\sqrt{N}}\sum_k a_k e^{ikl}\ ,\\ a^\dagger_l&=\frac{1}{\sqrt{N}}\sum_k a^\dagger_k e^{-ikl}\ . \end{aligned} \quad (28)$$

The main limitation of the bosonization is that while for a given spin S^z_l can only assume $2S+1$ values, the corresponding boson operators can take an infinite number of states. This difference leads to what Dyson called the kinematical interaction. It can be taken into account by projecting out all the unphysical states. The kinematical interaction becomes less important with increasing spin. In our case, since we are interested in the classical limit, which corresponds to $S=\infty$, the kinematical interaction can be neglected altogether. Moreover, it has been shown[28] that the Dyson-Maleev bosonization gives the exact result for $S_{00}(q'\omega)$ at $T=0$ even for spin $\frac{1}{2}$.

In terms of the boson operators, Hamiltonian (1) reads

$$H=E_0+\sum_k \hbar\omega_k a_k^\dagger a_k+\frac{1}{N}\sum_{k_1,k_2,q'} a^\dagger_{q'/2+k_1}a^\dagger_{q'/2-k_1}a_{q'/2+k_2}a_{q'/2-k_2}\hbar^2 V(k_1,k_2,q'/2)\ , \tag{29}$$

where

$$E_0=-JN\hbar^2S^2-ND\hbar^2S^2\left[1-\frac{1}{2S}\right]-Nh\hbar S\ , \tag{30}$$

$$\omega_k=\left[2J\hbar S\left[1-\frac{1}{g}\cos k\right]-h+2\hbar SD\left[1-\frac{1}{2S}\right]\right]\ , \tag{31}$$

$$V\left[k_1,k_2,\frac{q'}{2}\right]=\left[-J\cos k_2\left[\cos k_1-\frac{1}{g}\cos\frac{q'}{2}\right]-D\left[1-\frac{1}{2S}\right]\right]\ . \tag{32}$$

The factor $1-1/2S$ appearing in the single-site anisotropy term, ensuring that it vanishes for $S=\frac{1}{2}$, is obtained in a straightforward way from the Dyson-Maleev bosonization for the magnon energy ϵ_k. For the interaction term V, a more elaborate analysis is needed (see Ref. 40). In the classical limit ($S\to\infty$), the correction $1/2S$ vanishes. The variables A and S^x can be written in the form

$$S^x=\tfrac{1}{2}(S^++S^-)\ , \tag{33}$$

$$A=\frac{1}{\sqrt{2}}(S^+S^++S^-S^-)\ . \tag{34}$$

S^+ and S^- are Hermitian conjugates to each other, $(S^-)^\dagger=S^+$.

The identity

$$G_{A^\dagger B^\dagger}(\omega)=G^*_{AB}(-\omega) \tag{35}$$

($\dagger$ and * denote Hermitian and complex conjugation, respectively) allows us to write

$$\begin{aligned}G_{xx}(\omega)&=\tfrac{1}{4}\langle\langle S^++S^-;S^-+S^+\rangle\rangle\\&=\tfrac{1}{4}[\langle\langle S^+;S^-\rangle\rangle(\omega)+\langle\langle S^+;S^-\rangle\rangle^*(-\omega)]\ ,\end{aligned} \tag{36}$$

$$\begin{aligned}G_{AA}(\omega)&=\tfrac{1}{2}\langle\langle(S^+S^++S^-S^-);(S^-S^-+S^+S^+)\rangle\rangle\\&=\tfrac{1}{2}[\langle\langle S^-S^-;S^+S^+\rangle\rangle(\omega)\\&\quad+\langle\langle S^-S^-;S^+S^+\rangle\rangle^*(-\omega)]\ .\end{aligned} \tag{37}$$

It is thus sufficient to calculate the Green's function corresponding to one of the summands in (37), which we shall denote by $\bar{G}_{AA}$,

$$G_{AA}(\omega)=\tfrac{1}{2}[\bar{G}_{AA}(\omega)+\bar{G}^*_{AA}(-\omega)]\ . \tag{38}$$

The spin Green's functions can be expressed in terms of boson Green's functions,

$$\langle\langle S_l^+;S_j^-\rangle\rangle=2S\hbar^2\langle\langle a_l^\dagger;a_j\rangle\rangle-\hbar^2\langle\langle a_l^\dagger a_l^\dagger a_l;a_j\rangle\rangle\ . \tag{39}$$

Calculation of the two-boson Green's function using its equation of motion in the renormalized spin-wave approximation leads to the following expression for $S_{xx}(q,\omega)$ (Ref. 36):

$$\begin{aligned}S_{xx}(q,\omega)=\frac{1}{2}\frac{ST}{\omega}[&\delta(\omega-\omega_q(T))\\&+\delta(\omega+\omega_q(T))]\ ,\end{aligned} \tag{40}$$

where $\omega_q(T)$ is the temperature renormalized magnon frequency

$$\omega_q(T)=\omega_q+\Delta\omega_q(T)=\omega_q+a(T)+b(T)\cos q\ , \tag{41}$$

$$a(T)=T\left[-\frac{1}{S}+\left[\frac{K}{2S}-(2J+4D)\right]\times\frac{1}{[(K^2/4)-(4J^2S^2/g^2)]^{1/2}}\right]\ , \tag{42}$$

$$b(T)=T\left[\frac{g}{s}-\left[\frac{gK}{2S}-\frac{2J}{g}\right]\times\frac{1}{[(K^2/4)-(4J^2S^2/g^2)]^{1/2}}\right]\ , \tag{43}$$

$$K=4JS+2h+4DS\ .$$

Results for the spin-wave damping for the AEH have recently been reported by Lovesey.[41] The four-spin Green's function can be expressed as

$$\langle\langle S_l^- S_m^-; S_i^+ S_j^+ \rangle\rangle = 4S^2\hbar^4 \left[1-\frac{\delta_{ij}}{2S}\right] \langle\langle a_l a_m; a_i^\dagger a_j^\dagger \rangle\rangle - 2S\hbar^4 \langle\langle a_l a_m; a_i^\dagger a_j^\dagger a_j^\dagger a_j \rangle\rangle$$
$$-2S\hbar^4 \langle\langle a_l a_m; a_i^\dagger a_i^\dagger a_j^\dagger a_i \rangle\rangle + \hbar^4 \langle\langle a_l a_m; a_i^\dagger a_i^\dagger a_i a_j^\dagger a_j^\dagger a_j \rangle\rangle \ . \quad (44)$$

The three last terms are 1 or 2 orders higher in T than the first term. For low temperatures, we can make the approximation

$$\langle\langle S_l^- S_m^-; S_i^+ S_j^+ \rangle\rangle \simeq 4S^2\hbar^4 \left[1-\frac{\delta_{ij}}{2S}\right] \langle\langle a_l a_m; a_i^\dagger a_j^\dagger \rangle\rangle \ , \quad (45)$$

which is also consistent with the decoupling approximation used to calculate $\langle\langle a_l a_m; a_i^\dagger a_j^\dagger \rangle\rangle$. In the classical limit, we obtain

$$\langle\langle S_l^- S_m^-; S_i^+ S_j^+ \rangle\rangle \approx 4S_{\rm cl}^2\hbar^2 \langle\langle a_l a_m; a_i^\dagger a_j^\dagger \rangle\rangle \ . \quad (46)$$

The remaining $\hbar^2$ is compensated by a factor $1/\hbar$ appearing in $\langle\langle a_l a_m; a_i^\dagger a_j^\dagger \rangle\rangle$ and by a factor from (19), leading to a well-defined finite expression for $S_{jj}(q,\omega)$.

The solution of the equation of motion for the four-boson Green's function is given in the Appendix. The method is based on a decoupling scheme for the six-boson term, representing a low-magnon density approximation, which becomes exact at $T=0$. Its range of validity for finite temperatures can be estimated by comparison with the molecular-dynamics calculation.

The explicit expressions for the form factors in the classical limit are given by

$$S_{jj} = 4S^2 \frac{T}{\omega} [G_{jj}^{b''}(q,\omega) - G_{jj}^{b''}(q,-\omega)] \ , \quad (47)$$

$$G_{00}^b(q,\omega) = \frac{G^0(1+2\pi JR) - 2\pi JCB_1}{1+L} \ , \quad (48)$$

$$G_{11}^b(q,\omega) = \frac{B_2 + 2\pi D(G^0 B_2 - B_1^2)}{1+L} \ , \quad (49)$$

where

$$G^0(q,\omega) = \frac{1}{N} \sum_p \tilde{G}_{pp}^0(q,\omega) \ , \quad (50)$$

$$B_n(q,\omega) = \frac{1}{N} \sum_p \tilde{G}_{pp}^0 \cos^n p \ , \quad (51)$$

$$C(q,\omega) = B_1(q,\omega) - \frac{1}{g}\cos\frac{q}{2} G^0(q,\omega) \ , \quad (52)$$

$$R(q,\omega) = B_2(q,\omega) - \frac{1}{g}\cos\frac{q}{2} B_1(q,\omega) \ , \quad (53)$$

$$1+L(q,\omega) = (1+2\pi DG^0)(1+2\pi JR) - 4\pi^2 JDCB_1 \ . \quad (54)$$

At low T the form factors $S_{00}(q,\omega)$ and $S_{11}(q,\omega)$ have a contribution that extends between $\omega_{BC}(T)$ and $\omega_{TC}(T)$ related to the continuum, and one (AEH) or two (EAH) δ-function resonances corresponding to the two-magnon bound states. The relation between the resonances at finite low T in the classical limit and in the quantum-mechanical spectrum is the following. In the quantum treatment at $T=0$, the poles of G_{00} or G_{11} give the complete two-magnon spectrum consisting of a continuum of scattering states $\omega_{BC} \le \omega \le \omega_{TC}$, and bound states located at the zeros of

$$1+L'(q,\omega) = 0 \ . \quad (55)$$

For $T>0$, in the decoupling approximation, the structure of the integral equation (A18) is the same as for $T=0$. Therefore, the poles appear as continuum and discrete points, which are related to the quantum-mechanical spectrum by a temperature-dependent shift. The structure does not change when the classical limit is taken, and we can relate the classical resonances to the quantum spectrum. On this basis, we loosely use the denomination of continuum and bound states also found in the classical limit at $T>0$. According to the semiclassical correspondence, in the classical limit the bound-state contributions can be identified as envelope-soliton effects. An important difference between the quantum and the classical results is that the classical form factors at $T=0$ are identically zero, i.e., all the resonances are thermally induced.

Figure 1 shows the location of the bound-state

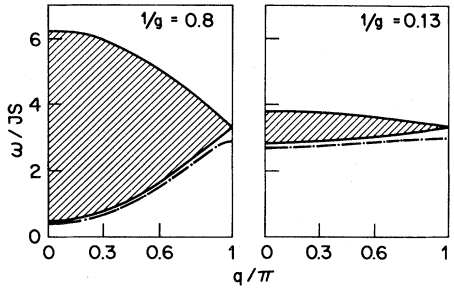

FIG. 1. Location of the two-magnon bound state (—·—) and continuum in the classical limit for the AEH at $T^*=0.33$, $h^*=0$.

resonance and the two-magnon continuum of the AEH, as given by Eqs. (55) and (56), at $T^*=T/JS^2=0.33$. We have taken a small anisotropy $1/g=0.8$, such that at long wavelengths the system is close to the continuum model, and a larger anisotropy $1/g=0.13$. The gap between the continuum and the bound state as it appears in the decoupling approximation increases with the anisotropy, thus allowing a better resolution of the resonances. The temperature dependence of the gap goes classically as[28,42]

$$\omega_{BC}(T)-\omega_B(T)\sim\begin{cases}T^2 & \text{for } q\neq\pi\\ T & \text{for } q=\pi\ .\end{cases} \tag{56}$$

This gives us an indication that at low T the bound-state resonance will be difficult to resolve from the continuum. On the other hand, if the temperature is raised, broadening of the resonances prevents a good resolution. However, in the AEH model, evaluation of Eq. (49) shows that the contribution of the continuum to $S_{11}(q,\omega)$ vanishes at $q=\pi$:

$$S_{11}(\pi,\omega)=a_1\delta(\omega-\omega_B)\ , \tag{57}$$

where

$$a_1=8\frac{T^2}{\omega}\frac{K}{Q'^2}\left[1-\left[1-\frac{Q'^2}{K^2}\right]^{1/2}\right], \tag{58}$$

and ω_B is the bound-state frequency

$$\omega_B=-\tilde{K}+8TJ\frac{K}{Q'^2}\left[1-\left[1-\frac{Q'^2}{K^2}\right]^{1/2}\right]. \tag{59}$$

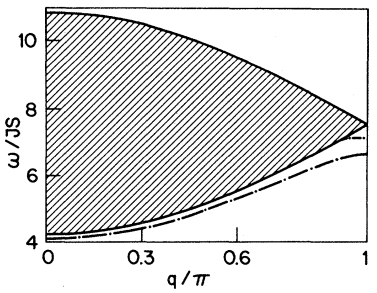

FIG. 2. Location of the two-magnon bound states ($-\cdot-$) and continuum in the classical limit for the EAH at $T^*=1$, $h^*=1$, $D^*=1$.

[Q, Q', $\tilde{K}$, and K are defined in (A21)–(A25).]

Thus at low temperatures $S_{11}(\pi,\omega)$ for the AEH will consist of a single peak related to the bound state. This is very well confirmed by the MD results (Fig. 6). For $q\neq\pi$, the resolution of the bound state is improved for increasing anisotropy g. Then, however, the system is further away from the continuum limit. The interpretation of the classical bound-state resonances as soliton effects is still justified by the fact that the structure of the form factors remains unchanged when the anisotropy is increased.

For the EAH the situation is similar, as shown in Fig. 2. In this case, a second bound state appears close to the zone boundary.[8,9] For realistic values of the single-site anisotropy the EAH shows stronger resolution problems than the AEH.

It is interesting to compare (48) and (49) with the classical linear spin-wave theory results, obtained by neglecting the magnon interaction, i.e., by setting $V=0$ in (29):

$$S^0_{00}(q,\omega)=\frac{32T^2S^2}{\pi}\frac{1}{[\omega^2-\tan^2(q/2)(\omega-\omega_{BC})(\omega_{TC}-\omega)][(\omega-\omega_{BC})(\omega_{TC}-\omega)]^{1/2}}\ , \tag{60}$$

$$S^0_{11}(q,\omega)=S^0_{00}\cos^2 b$$

$$=\frac{2T^2g^2}{\pi J^2}\frac{(\omega+4JS+2h+4DS)^2}{[\cos^2(q/2)\omega^2-\sin^2(q/2)(\omega-\omega_{BC})(\omega_{TC}-\omega)][(\omega-\omega_{BC})(\omega_{TC}-\omega)]^{1/2}}\ , \tag{61}$$

where ω_{BC} and ω_{TC} are given by (24) and (25). Both S^0_{00} and S^0_{11} have square-root singularities at the top and bottom of the continuum. By taking into account the interaction, these unphysical singularities disappear and the bound-state resonances appear. The rounding-off of the singularities by the interaction is already found in the quantum model at $T=0$, where S_{jj} can be calculated exactly, which confirms their unphysical character. In this respect, these singularities differ from the ones found, e.g., in the $S=\frac{1}{2}$ XY model, which have a physical nature and appear even at finite temperatures. Their appearance there is to be attributed to the equivalence of the XY model to a gas of noninteracting fermions.

V. COMPARISON WITH MOLECULAR DYNAMICS

The theory developed in the previous sections is expected to be valid for low temperatures. We com-

pare these predictions with numerical molecular-dynamics (MD) calculations for the following purposes: First, we want to check the range of validity of the theory and specifically of the decoupling scheme (A12). Furthermore, we know that the bound-state δ-function resonances, as well as the boundaries of the continuum, will be broadened at any finite T. We use the numerical results to check to what extent the bound-state resonances can be resolved from the continuum. Finally, we investigate whether some new phenomena appear at higher temperatures where the theory is no longer valid. The criterion to identify envelope-soliton effects in the dynamic form factors is based on the following considerations: In the preceding section, we have seen that the bound-state resonance in $S_{jj}(q,\omega)$ survives the classical limit. The identification of semiclassically quantized envelope solitons with magnon bound states provides a natural interpretation of these resonances as soliton effects. This criterion can be applied to any bound-state-originated resonances that survive in the classical limit.

Checking the validity of the decoupling scheme is important, since, due to the absence of long-range order at $T>0$, its applicability is not guaranteed. It is known, for example, that in the isotropic Heisenberg model, in zero field the Dyson-Maleev bosonization combined with a similar decoupling scheme does not reproduce the symmetry of the form factors in the x, y, and z directions. In the AEH and EAH the axial anisotropy avoids this problem. In spite of the absence of long-range order in one dimension at finite T, the existence of well-defined spin-wave resonances has been established.[43-47] This can be explained by the strong short-range order at low T, characteristic of one-dimensional systems.

The good agreement at low T between the molecular-dynamics and the theoretical results calculated using the decoupling scheme (e.g., Figs. 3 and 6), even in the absence of an external field, is also to be attributed to the presence of this strong short-range order. For higher temperatures some modifications must be expected due to scattering of the magnons on the boundaries of the domains of different mean orientation, and, in general, to higher-order processes.

We give only a very schematical description of the molecular-dynamics technique. A more complete account can be found in Refs. 44–49 and in Ref. 6. The method used for the present calculations is based on the numerical solution of the equation of motion (8) for a finite chain of N classical spin with periodic boundary conditions. The algorithm used has the advantage of being stable over long integration times.[44-47]

A set of initial configurations, such that they are representatives of a canonical ensemble, is constructed using a Monte Carlo procedure. Then, each of the initial configurations is allowed to evolve completely deterministically according to (8). From the data time-dependent correlations are calculated by averaging over the initial conditions. Finally, the dynamical form factors are obtained by Fourier transformation.[49] They are smoothened by Gaussian convolution to eliminate oscillations produced by the finiteness of the chain and of the integration time. The finite integration time sets a limit to the resolution in ω. This means that the method would not be sensitive to long-time tail phenomena, since the long-time (small ω) behavior is taken from the Gaussian convolution. However, this does not affect the present calculations since we are looking at nonconserved, fast-relaxing variables at low temperatures that correspond to a collisionless, i.e., nonhydrodynamic regime.

The accuracy and convergence of the method has been checked for the isotropic Heisenberg model[44-46] by comparison with exactly known static properties.[34,50] An inner check and improvement of the results are obtained by taking longer chains, more initial configurations, and smaller time steps.

In our calculations we used chains of length $N=1000$ spins and 20 different starting configurations for each set of parameters. The seed configuration for the Monte Carlo thermalization was taken completely ordered or completely random, leading to the same results in both cases. The convergence of the method was heuristically checked by comparing with calculations on chains of length $N=50$ and 10 to 40 starting configurations which could already reproduce the results of the larger systems. In general, MD, in a way similar to any experimental measurement, give accurate results for the positions of the resonance peaks, while their heights are subject to stronger variations due mainly to statistic and resolution effects.

We begin by discussing some results for the EAH. The parameters are given in reduced units, $T^*=T/JS^2$, $h^*=h/JS$, $D^*=D/J$, $\omega^*=\omega/JS$. We consider a low and a higher temperature. The range of validity of the approximate theory depends on the type and strength of the anisotropy, as well as on the applied field. Figure 3(a) shows $S_{00}(q=0,\omega)$ at $T^*=0.1$. The theoretical curve calculated from Eqs. (47) and (48) agrees very well

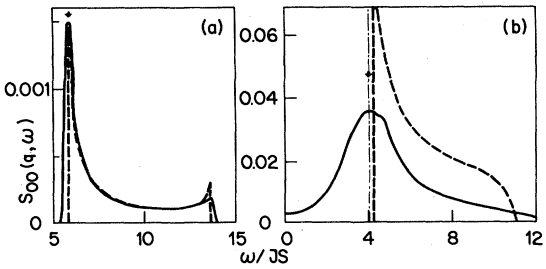

FIG. 3. $S_{00}(q,\omega)$ for the EAH at $q=0$, $h^*=1$, $D^*=1$ and (a): $T^*=0.1$, (b): $T^*=1$. MD: ——; theory: — — — (continuum); —·— and ↓ (bound state).

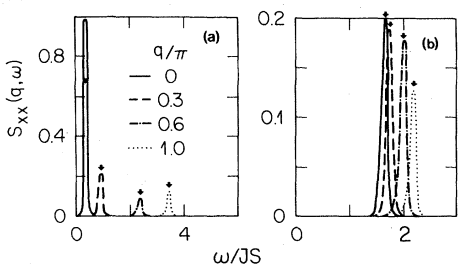

FIG. 5. $S_{xx}(q,\omega)$ for the AEH at $T^*=0.1$, $h^*=0$. (a) $1/g=0.8$, (b) $1/g=0.13$. The arrows indicate the renormalized spin-wave frequencies.

with the MD curve. The bound-state resonance cannot be resolved from the continuum. Figure 3(b) shows $S_{00}(0,\omega)$ for the same parameters at a higher temperature $T^*=1$. The difference between the theoretical and MD curves is already quite pronounced. However, the location of the bound-state resonance coincides accurately with the peak maximum. Figure 4 shows $S_{xx}(q,\omega)$ for $T^*=1$. Although the magnon peaks are already quite broad, their location agrees with the renormalized spin-wave frequency (41).

For the AEH, we have chosen two different anisotropy parameters, $1/g=0.8$ and $1/g=0.13$. For $1/g=0.8$ the system is, at long wavelengths, close to the continuum model, and the interpretation of bound-state contributions as soliton effects is very direct. For the larger anisotropy $1/g=0.13$ the structure of the resonances is qualitatively the same, but the resolution is better, and the resonances are better defined because the dispersion curves are less steep. The interpretation of the bound-state contributions as soliton features is more indirect, based on their qualitative invariance as a function of the anisotropy. Figure 5 shows $S_{xx}(q,\omega)$ at a low temperature $T^*=0.1$. The location of the magnon resonances agrees with the renormalized spin-wave prediction.

Figure 6 shows $S_{11}(q,\omega)$ at $T^*=0.1$, $q=0$, and $q=\pi$. For $1/g=0.8$, $q=0$, the bound state is so close to the continuum that it cannot be resolved at all. For $1/g=0.13$, $q=0$, the left-peak maximum coincides very accurately with the location of the bound-state resonance. Its height and width are about twice the theoretical continuum prediction. The difference is produced by the bound-state resonance. For both anisotropies, at $q=\pi$ there is a single resonance at the bound-state frequency, as predicted by Eq. (57), since the continuum contribution vanishes in leading order in T. This gives the most clear-cut bound-state or soliton effect, due to the absence of any resolution problems. Figure 7 shows $S_{00}(q,\omega)$ at $T^*=0.1$. The main contribution to the left peak comes from the bound state. For $q=0.6\pi$ it appears even clearer since the continuum gives rise essentially to only one peak.

We now look at a higher temperature $T^*=0.33$, at which important deviations from the approximate theory are already present. The position of the bound-state resonance in $S_{11}(q,\omega)$ is still correctly predicted, but the continuum contribution is much smaller than predicted. Moreover, a new feature, a central peak around $\omega=0$, appears (Fig. 8), which is unexpected from the low-temperature theory. A similar effect is found for $S_{00}(q,\omega)$ (Fig.

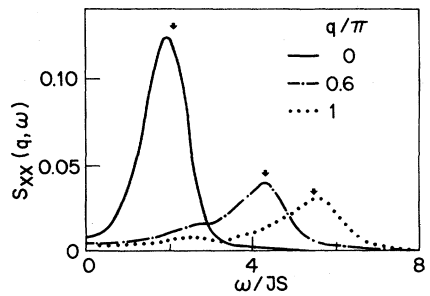

FIG. 4. $S_{xx}(q,\omega)$ for the EAH at $T^*=1$, $h^*=1$, $D^*=1$. The arrows indicate the renormalized spin-wave frequencies.

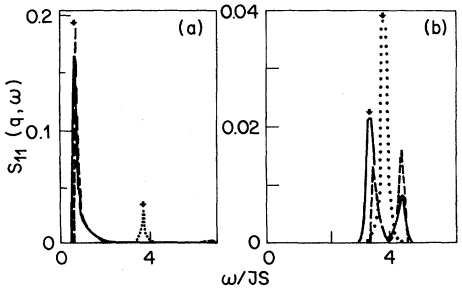

FIG. 6. $S_{11}(q,\omega)$ for the AEH at $T^*=0.1$, $h^*=0$. (a) $1/g=0.8$, (b) $1/g=0.13$. $q=0$: MD: ——; theory: — — — (continuum), ↓ (bound state). $q=\pi$: ·····.

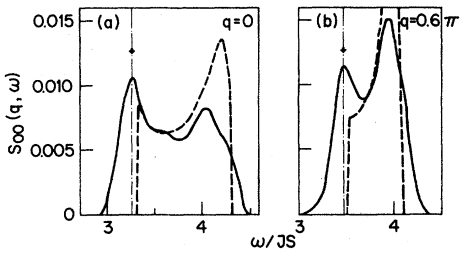

FIG. 7. $S_{00}(q,\omega)$ for the AEH at $T^*=0.1$, $h^*=0$. (a) $1/g=0.8$, (b) $1/g=0.13$. MD: ——; theory: – – – (continuum); —·— and ↓ (bound state).

9) and for $S_{xx}(q,\omega)$ (Fig. 10).

The origin of these thermally-induced central peaks can be understood by the following comparison with recent quantum $S=\frac{1}{2}$ finite-chain calculations,[51,52] where they have also been observed. In this approach the Hamiltonian corresponding to chains of eight to twelve spins is diagonalized numerically, yielding the eigenvalues and eigenvectors. On this basis, the form factors can be calculated explicitly, thereby allowing an analysis of the peak structure in terms of the underlying transitions. The central peak appearing in $S_{xx}(q,\omega)$ at $T^*=0.33$ was traced back to the transitions $\omega_1\to\omega_2$, $\omega_2\to\omega_3$, and $\omega_3\to\omega_4$. $\omega_n\to\omega_m$ denotes a transition between an n-magnon and an m-magnon bound state. In $S_{11}(q,\omega)$ the central peak is produced mainly by the transitions $\omega_1\to\omega_3$ and $\omega_2\to\omega_4$. Comparison with the classical results shows that these resonances survive in the classical limit. There, these processes correspond, according to semiclassical quantization arguments, to collisions involving envelope solitons. Thus the central peaks observed in the classical form factors S_{xx}, S_{11}, and S_{00} can be identified as soliton effects. They do not appear in our low-temperature theory because the decoupling schemes exclude higher-order bound-state contributions.

The dispersion of the m-magnon bound state for

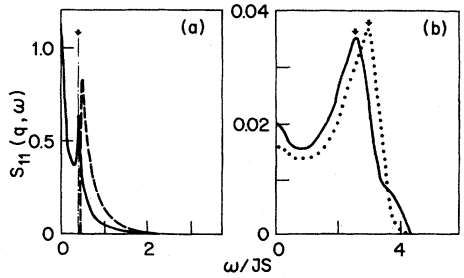

FIG. 8. $S_{11}(q,\omega)$ for the AEH at $T^*=0.33$, $h^*=0$. (a) $1/g=0.8$, $q=0$. MD: ——; theory: – – – (continuum), —·— ↓ (bound state). (b) $1/g=0.13$. MD: —— $q=0$, ····· $q=\pi$; theory: ↓ (bound state).

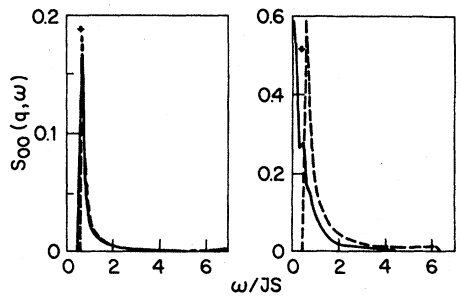

FIG. 9. $S_{00}(q,\omega)$ at $q=0$, $1/g=0.8$, $h^*=0$. MD: ——; theory: – – – (continuum), ↓ (bound state). (a) $T^*=0.1$, (b) $T^*=0.33$.

$S=\frac{1}{2}$ is given by[26]

$$\omega_m(q)=\frac{J}{g}\frac{\sinh\phi}{\sinh m\phi}(\cosh m\phi-\cos q)+mh\ ,$$
$$\cosh\phi=g\ . \tag{62}$$

For $h=0$ and large m, $\omega_m(q)$ becomes independent of q and goes to the limit

$$\lim_{m\to\infty}\omega_{m,q}=J(1-1/g^2)^{1/2}\ . \tag{63}$$

For large anisotropies (e.g., $1/g=0.13$), this limit is almost reached already for small m ($m\approx 3$). The energy difference between the bound states is small and q independent, which explains why the the transitions among them give rise to a central peak. For small anisotropies (e.g., $1/g=0.8$), the asymptotic value (63) and the q independence are reached only for higher m ($m\approx 7$). This produces a much broader central peak as well as stronger broadening of the one- and two-magnon resonances.

The effect of a magnetic field h on the form factors can be predicted from the dependence of the m-magnon bound-state energy on h [Eq. (62)]. The field shifts the branches by mh, so that asymptotically, $\omega_m\to J(1-1/g^2)^{1/2}+mh$. For low T the field will only shift the resonances in S_{xx} and S_{jj}. For a higher temperature (e.g., $T^*=0.33$), a strong

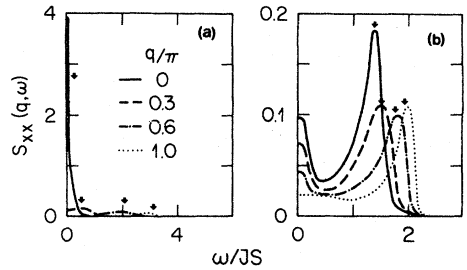

FIG. 10. $S_{xx}(q,\omega)$ at $T^*=0.33$, $h^*=0$. ↓ renormalized spin-wave frequencies. (a) $1/g=0.8$, (b) $1/g=0.13$.

enough field will cause the disappearance of the central peak, because the higher energy gap will lower the occupation of the excited states. Therefore, we can expect an applied field to extend the validity of our low-temperature theory. This is confirmed by the MD calculation for S_{xx}, S_{11}, and S_{00} as shown in Fig. 11 for S_{11}. A further consequence is that when the transitions between bound states acquire observable thermal weight, their contributions to the central peak will be shifted by $\sim\Delta mh$, producing a broadening or even splitting of the central peak. This splitting effect has been observed[53] in a recent finite-chain calculation for $S=\frac{1}{2}$.

The close similarity between the $S=\frac{1}{2}$ and the classical ($S=\infty$) form factors suggests that the essential features of the thermally-induced resonance structures in AEH ferromagnets are independent of the spin value. This view is supported by the results at $T=0$ (QM), where the form factors can be calculated exactly for all spin values.[28] Changes in S produce only minor quantitative differences. This fact must be attributed to the simplicity of the ground state in axial anisotropic ferromagnets. For systems with more complicated ground states, e.g., with planar anisotropy (where no exact results are known, even at $T=0$), preliminary numerical results[54] show a strong dependence on the spin value.

In conclusion, we have seen that the classical limit of magnon bound states, and thus the envelope solitons, produce several important effects in the dynamical form factors of axial anisotropic Heisenberg ferromagnetic chains: At low T there is a two-magnon bound-state resonance in $S_{00}(q,\omega)$ and $S_{11}(q,\omega)$ which is difficult to resolve, except at $S_{11}(q=\pi,\omega)$ in the AEH, where it is the dominant contribution. At higher temperatures, magnon bound states are responsible for the central peaks observed in $S_{xx}(q,\omega)$, $S_{00}(q,\omega)$, and $S_{11}(q,\omega)$. Finally, the qualitative invariance of the form factors for spin values ranging from $\frac{1}{2}$ to ∞ supports the interpretation in terms of envelope soliton features of experiments on quasi-one-dimensional axial anisotropic ferromagnets with $S>\frac{1}{2}$.

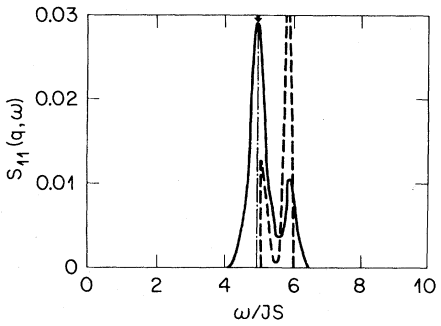

FIG. 11. $S_{11}(q,\omega)$ at $T^*=0.33$, $h^*=1$, $1/g=0.13$, $q=0$. MD: ——; theory: — — — (continuum), —·— ↓ (bound state).

ACKNOWLEDGMENTS

We should like to express our gratitude to J. M. Loveluck and E. Stoll, who wrote the original computer programs for the simulations, as well as to R. H. Swendsen, T. M. Rice, and A. Baratoff for helpful discussions and suggestions.

APPENDIX: SOLUTION OF THE EQUATIONS OF MOTION

We calculate $G_{00}(q,\omega)$ and $G_{11}(q,\omega)$ by solving the equation of motion of the corresponding two-boson Green's function

$$G_{pp'}(q,\omega)=\langle\langle a_{q/2+p}a_{q/2-p};a^{\dagger}_{q/2+p'}a^{\dagger}_{q/2-p'}\rangle\rangle\ , \tag{A1}$$

to which, for low T, they are related by

$$G_{jj}(q,\omega)=\tfrac{1}{2}[\bar{G}_{jj}(q,\omega)+\bar{G}^{*}_{jj}(q,-\omega)]\ , \tag{A2}$$

$$\bar{G}_{00}(q,\omega)\approx 4S^2\hbar^4\left[1-\frac{1}{2S}\right]G^{b}_{00}(q,\omega)\ , \tag{A3}$$

$$G^{b}_{00}(q,\omega)=\frac{1}{N}\sum_{pp'}G_{pp'}(q,\omega)\ , \tag{A4}$$

$$\bar{G}_{11}(q,\omega)\approx 4S^2\hbar^4G^{b}_{11}(q,\omega)\ , \tag{A5}$$

$$G^{b}_{11}(q,\omega)=\frac{1}{N}\sum_{pp'}\cos p\,G_{pp'}(q,\omega)\cos p'\ . \tag{A6}$$

The equation of motion of $G_{pp'}(q,\omega)$ is

$$\hbar\omega G_{pp'}=\frac{\hbar}{2\pi}\langle[a_{q/2+p}a_{q/2-p},a^{\dagger}_{q/2+p'}a^{\dagger}_{q/2-p'}]\rangle+\langle\langle[a_{q/2+p}a_{q/2-p},H];a^{\dagger}_{q/2+p'}a^{\dagger}_{q/2-p'}\rangle\rangle\ . \tag{A7}$$

The first commutator yields

$$\langle[a_{q/2+p}a_{q/2-p},a^{\dagger}_{q/2+p'}a^{\dagger}_{q/2-p'}]\rangle=(\delta_{p,p'}+\delta_{p,-p'})(1+n_{q/2+p}+n_{q/2-p})\ , \tag{A8}$$

where n_k are Bose occupation numbers

$$n_k = \langle a_k^\dagger a_k \rangle = (l^{\beta\omega_k} - 1)^{-1} . \tag{A9}$$

The classical limit gives

$$\lim_{\substack{\hbar \to 0,\ S \to \infty \\ \hbar S = S_{\rm cl}}} \hbar n_k = \frac{T}{\omega_k} . \tag{A10}$$

The second term yields

$$\begin{aligned} &\langle\langle [a_{q/2+p} a_{q/2-p}, H]; a_{q/2+p'}^\dagger a_{q/2-p'}^\dagger \rangle\rangle \\ &= \hbar(\omega_{q/2+p} + \omega_{q/2-p}) G_{pp'} + \frac{2}{N} \sum_{k_2} \hbar^2 V(p,k_2,q'/2) G_{k_2 p'} \\ &\quad + \frac{2}{N} \sum_{k_1,k_2,q'} \hbar^2 V(k_1,k_2,q'/2) (\delta_{q-p,q'+k_1} \langle\langle a_{q'-k_1}^\dagger a_{q+p} a_{q'+k_2} a_{q'-k_2}; a_{q+p'}^\dagger a_{q-p'}^\dagger \rangle\rangle \\ &\qquad + \delta_{q+p,q'+k_1} \langle\langle a_{q'-k_1}^\dagger a_{q-p} a_{q'+k_2} a_{q'-k_2}; a_{q+p'}^\dagger a_{q-p'}^\dagger \rangle\rangle) . \end{aligned} \tag{A11}$$

For low T the six-boson Green's function can be approximated in terms of four-boson functions using the following decoupling scheme:

$$\begin{aligned} &\delta_{q-p,q'+k_1} \langle\langle a_{q'-k_1}^\dagger a_{q+p} a_{q'+k_2} a_{q'-k_2}; a_{q+p'}^\dagger a_{q-p'}^\dagger \rangle\rangle \\ &\qquad \approx \delta_{q,q'} \delta_{p,-k_1} n_{q+p} G_{k_2 p'} + \delta_{q-p,q'+k_1} \delta_{k_1,-k_2} n_{q'-k_1} G_{pp'} + \delta_{q-p,q'+k_1} \delta_{k_1,k_2} n_{q'-k_1} G_{pp'} . \end{aligned} \tag{A12}$$

The second and third terms are proportional to $G_{pp'}$, and thus have only the effect of renormalizing $\omega_{q/2\pm p}$ in (A11). The decoupling scheme (A12) becomes exact at $T=0$, and we recover the exact solutions of Refs. 7 and 9. This shows further that the Dyson-Maleev bosonization gives exact results at $T=0$ for all spin values. The third term of (A11) becomes

$$\begin{aligned} &\hbar^2 (n_{q/2+p} + n_{q/2-p}) \frac{2}{N} \sum_{k_2} V(p,k_2,q/2) G_{k_2 p'} + \hbar^2 G_{pp'} \frac{4}{N} \sum_{k_1} V(k_1,k_1,q/2+p-k_1) n_{q/2+p-2k_1} \\ &\quad + \hbar^2 G_{pp'} \frac{4}{N} \sum_{k_1} V(k_1,k_1,q/2-p-k_1) n_{q/2-p-2k_1} . \end{aligned} \tag{A13}$$

We have used the symmetries $V(p,k,q) = V(-p,k,q)$ and $V(p,k_1,q) = V(p,-k_1,q)$. We insert (A7) into the equation of motion and introduce the shifted frequencies $\tilde{\omega}_k$:

$$G_{pp'} = \frac{1}{2\pi} (\delta_{p,p} + \delta_{p,-p'}) \frac{1 + n_{q/2+p} + n_{q/2-p}}{\omega - \tilde{\omega}_{q/2+p} - \tilde{\omega}_{q/2-p}} + \frac{2\hbar(1 + n_{q/2+p} + n_{q/2-p})}{\omega - \tilde{\omega}_{q/2+p} - \tilde{\omega}_{q/2-p}} \frac{1}{N} \sum_{k_2} V(p,k_2,q/2) G_{k_2 p'} \tag{A14}$$

with

$$\tilde{\omega}_{q/2\pm p} = \omega_{q/2\pm p} + \frac{4}{N} \sum_{k_1} \hbar V(k_1,k_1,q/2 \pm p - k_1) n_{q/2\pm p - 2k_1} . \tag{A15}$$

Setting $V=0$, we get the noninteracting spin-wave theory result

$$G_{pp'}^0 = \frac{\delta_{p,p'} + \delta_{p,-p'}}{2\pi} \frac{1 + n_{q/2+p} + n_{q/2-p}}{\omega - \omega_{q/2+p} - \omega_{q/2-p}} . \tag{A16}$$

We define $\tilde{G}_{pp'}^0$ as $G_{pp'}^0$, but including the shifted frequencies

$$\tilde{G}_{pp'}^0 = \frac{\delta_{p,p'} + \delta_{p,-p'}}{2\pi} \frac{1 + n_{q/2+p} + n_{q/2-p}}{\omega - \tilde{\omega}_{q/2+p} - \tilde{\omega}_{q/2-p}} . \tag{A17}$$

The equation for $G_{pp'}$ can be written as

$$G_{pp'} = \tilde{G}_{pp'}^0 + 2\pi\hbar \tilde{G}_{pp}^0 \frac{1}{N} \sum_{k_2} V(p,k_2,q/2) G_{k_2 p'} . \tag{A18}$$

The solution can be found performing the following steps: We obtain two coupled algebraic equations for $\sum_p G_{pp'}$ and $\sum_p \cos p\, G_{pp'}$ by summing (A18) over p for the first one, and by multiplying (A18) by $\cos p$ and then summing over p for the second one. Multiplication with $\cos p'$ and summation over p' gives us $G^b_{00}(q,\omega)$ and $G^b_{11}(q,\omega)$.

The frequency shift can be calculated explicitly in the classical limit. In the thermodynamical limit, $(1/N)\sum_{k_1}$ can be substituted by $(1/2\pi)\int_{-\pi}^{\pi} dk_1$. We introduce the following notation:

$$\omega_k = \frac{K}{2} - \frac{2JS}{g}\cos k \ , \tag{A19}$$

$$\omega_{q/2+p} + \omega_{q/2-p} = K + Q\cos p \ , \tag{A20}$$

$$K = 4JS + 2h + 4DS \ , \tag{A21}$$

$$Q = -\frac{4JS}{g}\cos\frac{q}{2}, \quad Q' = -\frac{4JS}{g}\sin\frac{q}{2} \ . \tag{A22}$$

After performing the integration, the shifted frequencies can be written in the simple form

$$\tilde{\omega}_{q/2+p} + \tilde{\omega}_{q/2-p} = \tilde{K} + \tilde{Q}\cos p \ , \tag{A23}$$

$$\tilde{K} = K - \frac{2T}{S}\left[\frac{4D(S-1)-2h}{[K^2-(4JS/g)^2]^{1/2}} + 1\right] , \tag{A24}$$

$$\tilde{Q} = Q + \frac{2Tg}{S}\left[\frac{(4JS/g^2)-K}{[K^2-(4JS/g)^2]^{1/2}} + 1\right]\cos\frac{q}{2} \ , \tag{A25}$$

$$G^b_{00}(q,\omega) = \frac{G^0(1+2\pi\hbar JR) - 2\pi\hbar JCB_1}{1+L} \ , \tag{A26}$$

$$G^b_{11}(q,\omega) = \frac{B_2 + 2\pi\hbar D(1-1/2S)(G^0 B_2 - B_1^2)}{1+L} , \tag{A27}$$

where

$$G^0(q,\omega) = \frac{1}{N}\sum_p \tilde{G}^0_{pp}(q,\omega) \ , \tag{A28}$$

$$B_n(q,\omega) = \frac{1}{N}\sum_p \tilde{G}^0_{pp'}(q,\omega)\cos^n p \ , \tag{A29}$$

$$C(q,\omega) = B_1(q,\omega) - \frac{1}{g}\cos\frac{q}{2}G^0(q,\omega) \ , \tag{A30}$$

$$R(q,\omega) = B_2(q,\omega) - \frac{1}{g}\cos\frac{q}{2}B_1(q,\omega) \ , \tag{A31}$$

$$\begin{aligned} 1+L(q,\omega) = {} & [1+2\pi\hbar D(1-1/2S)G^0] \\ & \times(1+2\pi\hbar JR) \\ & -4\pi^2\hbar^2 JD(1-1/2S)CB_1 . \end{aligned} \tag{A32}$$

The real and imaginary parts of the functions $G^0(q,\omega)$, $B_n(q,\omega)$, and thus $C(q,\omega)$, $R(q,\omega)$, and $L(q,\omega)$ can be evaluated explicitly in the classical limit.

Inspection of the formulas for $G^{b''}_{00}(q,\omega)$ and $G^{b''}_{11}(q,\omega)$ gives us the general structure of the form factors at low T:

$$\begin{aligned} G^{b''}_{00} = \{ & [G^{0'}(1+2\pi\hbar JR') - 2\pi\hbar JC'B'_1]L'' \\ & -[G^{0''}(1+2\pi\hbar JR') + 2\pi\hbar JG^{0'}R'' - 2\pi\hbar J(C''B'_1 + C''B'_1)](1+L')\}/[(1+L')^2 + L''^2] \ , \end{aligned} \tag{A33}$$

$$\begin{aligned} G^{b''}_{11} = \{ & -[(1+2\pi\hbar DG^{0'})B'_2 - 2\pi\hbar D(G^{0''}B''_2 + B'^2_1 - B''^2_1)]L'' \\ & +[B''_2 + 2\pi\hbar D(G^{0'}B''_2 + G^{0''}B'_2 - 2B'_1B''_1)](1+L')\}/[(1+L')^2 + L''^2] \ . \end{aligned} \tag{A34}$$

The imaginary parts F'' are nonzero in the continuum

$$0 < \tilde{\omega}_{BC} = \tilde{K} - |\tilde{Q}| \le \omega \le \tilde{K} + |\tilde{Q}| = \tilde{\omega}_{TC} \ .$$

Outside the continuum the F'' goes to zero proportionally to ϵ. There, $G^{b''}_{00}$ is of the form

$$\begin{aligned} G^{b''}_{00} &= \lim_{\epsilon\to 0}\frac{f_0\epsilon}{(1+L')^2+\epsilon^2} \\ &= f_0\delta(1+L'(q,\omega)) \end{aligned} \tag{A35}$$

and

$$\begin{aligned} G^{b''}_{11} &= \lim_{\epsilon\to 0}\frac{f_1\epsilon + f_2\epsilon^2 + f_3\epsilon^3}{(1+L')^2+\epsilon^2} \\ &= f_1\delta(1+L'(q,\omega)) \ . \end{aligned} \tag{A36}$$

Introducing into (A33) and (A34) the expressions for the functions G^0, B_n, C, R, and L, one sees that $G^{b''}_{jj}$ are of the form

$$G_{jj}^{b''}=\frac{1}{\hbar}\hat{G}_{jj}^{b''}\ , \tag{A37}$$

where $\hat{G}_{jj}^{b}$ depends only on the classical spin $S_{\rm cl}=S\hbar$.

The factors $1/\hbar$ cancel out when (A2), (A3), (A5), (A37), and (19) are combined to give $S_{jj}(q,\omega)$:

$$S_{jj}(q,\omega)=4S_{\rm cl}^2\frac{T}{\omega}\left[\hat{G}_{jj}^{b''}(q,\omega)-\hat{G}_{jj}^{b''}(q,-\omega)\right]\ . \tag{A38}$$

We note that for $\omega>0$ and $\omega<0$, the second and the first terms vanish, respectively.

[1]For reviews, see, for example, *Solitons,* edited by R. K. Bullough and P. J. Caudrey (Springer, Heidelberg, 1980); *Dynamical Systems,* Vol. 17 of *Lecture Notes in Physics* edited by J. Moser (Springer, Berlin, 1975); G. L. Lamb, Jr., *Elements of Soliton Theory (Wiley, New York, 1980).*

[2]H. Bethe, Z. Phys. 71, 205 (1931).

[3]L. A. Takhtadzhan and L. D. Faddeev, Russ. Math. Surv. 34, 11 (1979).

[4]P. P. Kulish and E. K. Sklyanin, Phys. Lett. 70A, 461 (1979).

[5]H. B. Thacker, Rev. Mod. Phys. 53, 253 (1981).

[6]E. Lieb, T. Schulz, and D. Mattis, Ann. Phys. (N.Y.) 16, 407 (1961).

[7]M. Wortis, Phys. Rev. B 2, 85 (1963).

[8]R. Silberglitt and J. B. Torrance, Phys. Rev. B 772 (1970).

[9]P. D. Loly and B. J. Choudhury, Phys. Rev. B 13, 4019 (1976).

[10]T. Schneider and E. Stoll, in *Structural Elements in Particle Physics and Statistical Mechanics,* edited by K. Fredenhagen and J. Honerkamp (Plenum, New York, 1982).

[11]M. Steiner, J. Villain, and C. G. Windsor, Adv. Phys. 25, 87 (1976).

[12]G. Shirane and R. J. Birgenau, Physica (Utrecht) 86, 639 (1977).

[13]L. J. de Jongh and A. R. Miedema, Adv. Phys. 23, 1 (1974).

[14]*Solitons and Condensed Matter Physics,* Vol. 8 of *Springer Series in Solid-State Sciences,* edited by A. R. Bishop and T. Schneider (Springer, Berlin, 1978).

[15]*Physics in One Dimension,* Vol. 23 of *Springer Series in Solid-State Sciences,* edited by J. Bernasconi and T. Schneider (Springer, Berlin, 1981).

[16]P. A. Fleury, in *Dynamical Properties of Solids,* edited by G. K. Horton and A. A. Maradudin (North-Holland, Amsterdam, 1980), Vol. 3.

[17]M. F. Thorpe, Phys. Rev. B 4, 1608 (1971).

[18]J. B. Torrance, Jr. and M. Tinkham, Phys. Rev. 187, 595 (1969).

[19]J. H. Mikeska, J. Phys. C 11, L29 (1978); 13, 1913 (1980).

[20]M. Steiner and J. K. Kjems, J. Phys. 10, 2665 (1977).

[21]J. M. Loveluck, T. Schneider, E. Stoll, and H. R. Jauslin, Phys. Rev. Lett. 45, 1505 (1980).

[22]J. M. Loveluck, T. Schneider, E. Stoll, and H. R. Jauslin, J. Phys. C 15, 1721 (1982).

[23]E. K. Sklyanin (unpublished).

[24]A. M. Kosevich, B. A. Ivanov, and A. S. Kovalev, Zh. Eksp. Teor. Fiz. Pis'ma Red. 25, 516 (1977) [Sov. Phys.—JETP Lett. 25, 486 (1977)].

[25]A. E. Borovik, Zh. Eksp. Teor. Fiz. Pis'ma Red. 28, 629 (1978) [Sov. Phys.—JETP Lett. 28, 629 (1978)].

[26]I. G. Gochev, Zh. Eksp. Teor. Fiz. 61, 1674 (1971) [Sov. Phys.—JETP 34, 892 (1972)].

[27]J. D. Johnson, S. Krinski, and B. M. McCoy, Phys. Rev. A 8, 2526 (1973).

[28]T. Schneider, Phys. Rev. B 24, 5327 (1981).

[29]B. A. Ivanov and A. M. Kosevich, Zh. Eksp. Teor. Fiz. 72, 2000 (1977) [Sov. Phys.—JETP 45, 1050 (1977)].

[30]A. M. Kosevich, B. A. Ivanov, and A. S. Kovalev, Fiz. Nizk. Temp. 3, 906 (1977) [Sov. J. Low Temp. Phys. 3, 44 (1977)].

[31]B. A. Ivanov, Fiz. Nizk. Temp. 3, 26 (1977) [Sov. J. Low Temp. Phys. 3, 505 (1977)].

[32]J. B. McGuire, J. Math. Phys. (N.Y.) 5, 622 (1964).

[33]M. Månson, Phys. Rev. B 12, 400 (1975).

[34]M. E. Fisher, Am. J. Phys. 32, 343 (1964).

[35]N. D. Mermin, J. Math. Phys. (N.Y.) 8, 1061 (1967); Phys. Rev. 134, A112 (1964).

[36]S. W. Lovesey, *Condensed-Matter Physics: Dynamic Correlations* (Benjamin, New York, 1980).

[37]G. Rickayzen, *Green's Functions and Condensed Matter* (Academic, New York, 1980).

[38]F. D. Dyson, Phys. Rev. 102, 1217 (1956); 102, 1230 (1956).

[39]S. V. Maleev, Zh. Eksp. Teor. Fiz. 33, 1010 (1957) [Sov. Phys.—JETP 6, 776 (1958)].

[40]U. Balucani, V. Tognetti, and M. G. Pini, J. Phys. C 12, 5513 (1979).

[41]S. L. Lovesey, Phys. Lett. 86A, 43 (1981).

[42]H. R. Jauslin, T. Schneider, E. Stoll, and J. M. Loveluck, J. Phys. C 15, L69 (1982).

[43]G. Reiter and A. Sjölander, Phys. Rev. Lett. 39, 1047 (1977); J. Phys. C 13, 3027 (1980).

[44]P. Heller and M. Blume, Phys. Rev. Lett. 39, 962 (1977).

[45]C. G. Windsor and J. Locke-Wheaton, J. Phys. C 9, 2749 (1976).

[46]J. M. Loveluck and C. G. Windsor, J. Phys. C 11, 2999 (1978).

[47]J. M. Loveluck and E. Balcar, Phys. Rev. Lett. 39, 962 (1977).

[48]T. Schneider and E. Stoll, Phys. Rev. B 17, 1302 (1978).

[49]R. Morf and E. Stoll, in *Numerical Analysis,* edited by

J. Descloux and J. Marti (Birkhäuser, Basle, 1977); Int. Ser. Num. Math. 37, 139 (1977).
[50]H. Tomita and H. Mashiyama, Prog. Theor. Phys. 48, 1133 (1972).
[51]T. Schneider and E. Stoll, Phys. Rev. Lett. 47, 377 (1981).
[52]T. Schneider and E. Stoll, Phys. Rev. B 25, 4721 (1982).
[53]T. Schneider and E. Stoll (unpublished).
[54]T. Schneider, E. Stoll, and U. Glaus, Phys. Rev. B 26, 1321 (1982).